

## Long-term evolution and gravitational wave radiation of neutron stars with differential rotation induced by $r$ -modes

Yun-Wei Yu <sup>\*</sup>, Xiao-Feng Cao, and Xiao-Ping Zheng

Institute of Astrophysics, Huazhong Normal University, Wuhan 430079, China

**Abstract** In a second-order  $r$ -mode theory, Sá & Tomé found that the  $r$ -mode oscillation in neutron stars (NSs) could induce stellar differential rotation, which leads to a saturation state of the oscillation spontaneously. Based on a consideration of the coupling of the  $r$ -modes and the stellar spin and thermal evolutions, we carefully investigate the influences of the  $r$ -mode-induced differential rotation on the long-term evolutions of isolated NSs and NSs in low-mass X-ray binaries, where the viscous damping of the  $r$ -modes and its resultant effects are taken into account. The numerical results show that, for both kinds of NSs, the differential rotation can prolong the duration of the  $r$ -mode saturation state significantly. As a result, the stars can keep nearly constant temperature and angular velocity over a thousand years. Moreover, due to the long-term steady rotation of the stars, persistent quasi-monochromatic gravitational wave radiation could be expected, which increases the detectibility of gravitational waves from both nascent and accreting old NSs.

**Key words:** stars: neutron — stars: evolution — stars: rotation — gravitational waves

### 1 INTRODUCTION

$R$ -modes in a perfect fluid star with arbitrary rotation arise due to the action of the Coriolis force with positive feedback (Andersson 1998; Friedman & Morsink 1998), succumbing to gravitational radiation-driven Chandrasekhar-Friedman-Schutz instability (Chandrasekhar 1970; Friedman & Schutz 1978). In contrast, the growth of the modes can be suppressed by the viscosity of the stellar matter. Thus the  $r$ -mode evolution is determined by the competition between the viscous damping effect and the destabilizing effect due to gravitational radiation. Based on the conservation of angular momentum, a phenomenological model describing the  $r$ -mode evolution was proposed by Owen et al. (1998) and improved by Ho & Lai (2000). However, since nonlinear effects are ignored in this original version of the model, an unbounded growth could lead the modes to an unphysical regime. By putting a saturation value for the  $r$ -mode amplitude into the model by hand, some authors (e.g., Owen et al. 1998; Levin 1999; Ho & Lai 2000; Watts & Andersson 2002; Heyl 2002) studied the spin and thermal evolutions and gravitational wave radiation of neutron stars (NSs).

To understand  $r$ -modes more deeply and judge their astrophysical implications, it is necessary to take into account some nonlinear effects that could give a saturation  $r$ -mode amplitude spontaneously (e.g., Schenk et al. 2002; Arras et al. 2003; Brink et al. 2004a, 2004b, 2005). As an important nonlinear effect, differential rotation induced by  $r$ -modes was first studied by Rezzolla et al. (2000, 2001) analytically using linearized fluid equations by expanding the velocity of a fluid element located at a certain point in powers of the mode amplitude, averaging over a gyration, and retaining only the lowest-order nonvanishing term. Soon afterwards, some numerical studies (Stergioulas & Font 2001; Lindblom et al.

---

<sup>\*</sup> E-mail: yuyw@phy.ccnu.edu.cn

2001) confirmed the existence of such drifts. More exactly, Sá (2004) solved the fluid equations within nonlinear theory up to the second order in the mode amplitude and described the differential rotation analytically. By extending the  $r$ -mode evolution model of Owen et al. (1998) to this nonlinear case, Sá & Tomé (2005, 2006) obtained a saturation amplitude of  $r$ -modes self-consistently. They also studied the early part (millions of seconds after the birth) of the spin evolution of nascent NSs under the influence of the differential rotation, but their calculation was not long enough to cover the phase during which the effect of the viscous damping of the  $r$ -mode operates. In this paper, we would find that the long-term spin and thermal evolution of isolated NSs and NSs in low-mass X-ray binaries (LMXBs) can also be remarkably influenced by the differential rotation by prolonging the duration of the  $r$ -modes. Moreover, in view of the prolonged  $r$ -modes, it can be accepted that gravitational waves would be continuously emitted from both young and accreting old NSs for a long time.

In the next section, we review the second-order  $r$ -mode theory of Sá (2004) briefly. Then, we exhibit the coupling thermal,  $r$ -mode, and spin evolution equations in Section 3, where some typical numerical solutions are given for both isolated and accreting NSs. In Section 4, we estimate the detectability of gravitational waves from NSs. Finally, a summary and discussion are given in Section 5.

## 2 THE SECOND-ORDER $R$ -MODES

For a rotating barotropic Newtonian star, the  $r$ -mode solutions of perturbed fluid equations can be found in spherical coordinates  $(r, \theta, \phi)$  at first order in  $\alpha$  as (Lindblom et al. 1998),

$$\delta^{(1)}v^r = 0, \quad (1)$$

$$\delta^{(1)}v^\theta = \alpha\Omega C_l l \left(\frac{r}{R}\right)^{l-1} \sin^{l-1} \theta \sin(l\phi + \omega t), \quad (2)$$

$$\delta^{(1)}v^\phi = \alpha\Omega C_l l \left(\frac{r}{R}\right)^{l-1} \sin^{l-2} \theta \cos \theta \cos(l\phi + \omega t), \quad (3)$$

and at second order in  $\alpha$  as (Sá 2004)

$$\delta^{(2)}v^r = \delta^{(2)}v^\theta = 0, \quad (4)$$

$$\begin{aligned} \delta^{(2)}v^\phi = & \frac{1}{2}\alpha^2\Omega C_l^2 l^2 (l^2 - 1) \left(\frac{r}{R}\right)^{2l-2} \sin^{2l-4} \theta \\ & + \alpha^2\Omega A r^{N-1} \sin^{N-1} \theta, \end{aligned} \quad (5)$$

where  $\alpha$  represents the amplitude of the oscillation,  $R$  and  $\Omega$  are the radius and angular velocity of the unperturbed star,  $\omega = -\Omega(l+2)(l-1)/(l+1)$ ,  $C_l = (2l-1)!!\sqrt{(2l+1)/[2\pi(2l)!(l+1)]}$ ,  $A$  and  $N$  are two constants determined by the initial condition. For simplicity, Sá & Tomé (2005) suggested  $N = 2l - 1$  and redefined  $A$  by introducing a new free parameter  $K$  as  $A = \frac{1}{2}KC_l^2 l^2 (l+1)R^{2-2l}$ . For the most unstable  $l = 2$   $r$ -mode of primary interest to us, the second-order solution  $\delta^{(2)}v^\phi$  shows a differential rotation of the star induced by the  $r$ -mode oscillation, i.e., large scale drifts of fluid elements along stellar latitudes. Using  $\delta^{(1)}v^i$  and  $\delta^{(2)}v^i$ , the corresponding Lagrangian displacements  $\xi^{(1)i}$  and  $\xi^{(2)i}$  can be derived and then the physical angular momentum of the  $l = 2$   $r$ -mode can be calculated up to the second order in  $\alpha$  as (Sá 2004; Sá & Tomé 2005)

$$J_r = J^{(1)} + J^{(2)} = \frac{(4K+5)}{2}\alpha^2 \tilde{J} M R^2 \Omega, \quad (6)$$

where  $\tilde{J} = 1.635 \times 10^{-2}$  and

$$J^{(1)} = - \int \rho \partial_\phi \xi^{(1)i} \left( \partial_t \xi_i^{(1)} + v^k \nabla_k \xi_i^{(1)} \right) dV, \quad (7)$$

$$\begin{aligned} J^{(2)} = & \frac{1}{\Omega} \int \rho v^i \left[ \partial_t \xi^{(1)k} \nabla_i \xi_k^{(1)} + v^k \nabla_k \xi^{(1)m} \nabla_i \xi_m^{(1)} + \partial_t \xi_i^{(2)} \right. \\ & \left. + v^k \left( \nabla_i \xi_k^{(2)} + \nabla_k \xi_i^{(2)} \right) \right] dV. \end{aligned} \quad (8)$$

Meanwhile, following Owen et al. (1998) and Sá (2004), we further express the energy of the  $l = 2$   $r$ -mode by

$$E_r = J^{(2)}\Omega - \frac{1}{3}J^{(1)}\Omega = \frac{(4K+9)}{2}\alpha^2\tilde{J}MR^2\Omega^2. \quad (9)$$

When  $K = -2$ ,  $J^{(2)}$  vanishes and the expressions of  $J_r$  and  $E_r$  return to their canonical forms (Owen et al. 1998), in other words, the differential rotation disappears. Both the physical angular momentum and energy of  $r$ -modes are increased by gravitational radiation back reaction and decreased by viscous damping, which yields

$$\frac{dJ_r}{dt} = \frac{2J_r}{\tau_g} - \frac{2J_r}{\tau_v}, \quad (10)$$

$$\frac{dE_r}{dt} = \frac{2E_r}{\tau_g} - \frac{2E_r}{\tau_v}, \quad (11)$$

where  $\tau_g = 3.26\tilde{\Omega}^{-6}$ s,  $\tau_{sv} = 2.52 \times 10^8 T_9^2$ s, and  $\tau_{bv} = 6.99 \times 10^8 T_9^{-6} \tilde{\Omega}^{-2}$ s are the timescales of the gravitational radiation, shear viscous damping, and bulk viscous damping (for  $l = 2$ ), respectively (Owen et al. 1998), and  $\tau_v = (\tau_{sv}^{-1} + \tau_{bv}^{-1})^{-1}$ . Hereafter, the convention  $Q_x \equiv Q/10^x$  and  $\tilde{\Omega} \equiv \Omega/\sqrt{\pi G \bar{\rho}}$  are adopted in cgs units. These timescales are obtained with a polytropic equation of state as  $p = k\rho^2$  for NSs, with  $k$  chosen so that the mass and radius of the star are  $M = 1.4M_\odot$  and  $R = 12.53$  km. The competition between the gravitational destabilizing effect that is dependent on  $\Omega$  and the  $T$ -dependent viscous damping effect determines an instability window in the  $T - \Omega$  plane, where a small perturbation would grow exponentially due to  $(\tau_g^{-1} - \tau_v^{-1})^{-1} > 0$ .

### 3 EVOLUTIONS OF NSS

#### 3.1 Thermal evolution equation

Considering the temperature dependence of the viscosities, we would like to show the thermal evolution equation of a NS first before calculating the  $r$  mode evolution, which reads (Shapiro & Teuklosky 1983; Yakovlev et al. 1999; Yakovlev & Pethick 2004)

$$\frac{dT}{dt} = -\frac{1}{C_v}(L_\nu + L_\gamma - H_{sv}), \quad (12)$$

where  $C_v \approx 10^{39}T_9$  erg K $^{-1}$  is the heat capacity of the star. On one hand, the NS can be cooled by neutrino and photon energy release, whose luminosities are estimated to be  $L_\nu \approx 10^{40}T_9^8$  erg s $^{-1}$  (for modified URCA process) and  $L_\gamma = 4\pi R^2\sigma T_s^4 \approx 10^{35}T_9^{2.2}$  erg s $^{-1}$ , respectively. For the blackbody luminosity  $L_\gamma$ , the relationship,  $T_s \approx 3.34 \times 10^6 T_9^{0.55}$ , between the interior ( $T$ ) and surface ( $T_s$ ) temperatures is used (Gudmundsson et al. 1983). Specifically, the temperature dependence of the luminosities indicates that the cooling of the NS at high ( $> 10^8$ K) and low ( $< 10^8$ K) temperatures would be dominated by neutrino and photon emissions, respectively. On the other hand, the shear viscous dissipation of  $r$ -modes can convert a part of the oscillation energy into heat energy gradually. Using the shear viscous damping timescale, the rate of this energy conversion can be estimated by

$$H_{sv} = \frac{2E_r}{\tau_{sv}} = 2.0 \times 10^{43}(4K+9)\alpha^2 T_9^{-2} \tilde{\Omega}^2 \text{ erg s}^{-1}. \quad (13)$$

For the very early ages of a nascent NS, during which this heating effect is much weaker than the neutrino cooling effect yet, an approximative temperature evolution can be solved from Eq. (12) as  $T = T_i(1+t/t_c)^{-1/6}$ , where  $T_i$  is the initial temperature and  $t_c \approx (20/T_{i,10}^6)$ s. However, as the  $r$ -modes increase, the cooling of the star would be resisted effectively by the heating effect, as demonstrated by some previous studies (e.g., Zheng et al. 2006).

### 3.2 Isolated NSs

A simple phenomenological model for  $r$ -mode evolution was proposed by Owen et al. (1998) first and further improved by Ho & Lai (2000) based on a consideration of angular momentum conservation. For a normal NS with a strong magnetic field ( $\sim 10^{10-12}$  G), besides the braking effect due to gravitational radiation, the spindown of the star resulting from magnetic dipole radiation should also be taken into account. So, we ought to write the decrease of the total angular momentum of the star as (Owen et al. 1998; Ho & Lai 2000; Sá & Tomé 2005)

$$\frac{dJ}{dt} = -\frac{3\alpha^2 \tilde{J} M R^2 \Omega}{\tau_g} - \frac{I \Omega}{\tau_m}, \quad (14)$$

where  $\tau_m = 1.35 \times 10^9 B_{12}^{-2} (\Omega / \sqrt{\pi G \bar{\rho}})^{-2}$  s is the magnetic braking timescale and  $I = \tilde{I} M R^2$  with  $\tilde{I} = 0.261$  is the moment of inertial of the star. Due to the  $r$ -mode oscillation, the total angular momentum of the star could be separated into two parts, i.e.,  $J = I\Omega + J_r$ . Then, Eqs. (10) and (14) yield

$$\frac{d\alpha}{dt} = \left[ 1 + \frac{4}{3}(K+2)Q\alpha^2 \right] \frac{\alpha}{\tau_g} - \left[ 1 + \frac{1}{3}(4K+5)Q\alpha^2 \right] \frac{\alpha}{\tau_v} + \frac{\alpha}{2\tau_m} \quad (15)$$

$$\frac{d\Omega}{dt} = -\frac{8}{3}(K+2)Q\alpha^2 \frac{\Omega}{\tau_g} + \frac{2}{3}(4K+5)Q\alpha^2 \frac{\Omega}{\tau_v} - \frac{\Omega}{\tau_m}, \quad (16)$$

where  $Q = 3\tilde{J}/2\tilde{I} = 0.094$ . During the very early ages of nascent NSs when  $\tau_g \ll (\tau_v, \tau_m)$ , the viscous and magnetic terms in the above two equations can be omitted. Combining this simplification with the analytical temperature  $T = T_i(1+t/t_c)^{-1/6}$ , Sá & Tomé (2005, 2006) obtained an analytical solution of Eqs. (15) and (16) for  $t < 0.1$  yr. For convenience, their analytical solution can also be expressed by two asymptotic functions as follows (Sá & Tomé 2006):

$$\alpha(t) \approx \begin{cases} \alpha_i \exp(t/\tau_{g,i}), & \text{for } t < t_a \\ \frac{3.56}{\sqrt{K+2}} (t/\tau_{g,i})^{1/10}, & \text{for } t > t_a \end{cases} \quad (17)$$

$$\Omega(t) \approx \begin{cases} \Omega_i \left[ 1 - \frac{4}{3}(K+2)Q\alpha_i^2 \exp(2t/\tau_{g,i}) \right], & \text{for } t < t_a \\ 0.63 (t/\tau_{g,i})^{-1/5}, & \text{for } t > t_a \end{cases} \quad (18)$$

where  $\alpha_i$  and  $\Omega_i$  are the initial  $r$ -mode amplitude and angular velocity, respectively, and  $\tau_{g,i} = 3.26\tilde{\Omega}_i^{-6}$  s. The transition time  $t_a \approx [521 - 18.5 \ln(K+2)]$  s corresponding to the amplitude of  $\alpha(t_a) = [12(K+2)Q]^{-1/2}$  is determined by the condition  $d^2\alpha/dt^2 = 0$  (Sá & Tomé 2006).

However, as the temperature and angular velocity decrease, the viscous damping timescale would become to be comparable to the gravitational radiation timescale. Therefore, it is necessary to completely solve the coupling Eqs. (12), (15), and (16) in order to depict the long-term history of NSs. For different values of  $K$  ( $\geq -5/4$ ), we show some numerical evolution curves of the  $r$ -mode amplitude in Figure 1. As indicated by the thin solid lines, the two increasing segments of the evolution curves can be fitted by Eq. (17) well, i.e., the amplitude increases rapidly first and then gradually reaches a saturation value. About one tenth year later after the birth of the stars, the growth of the  $r$ -mode would be stopped and instead, the amplitude nearly keeps constant until an extremely fast decay due to  $(\tau_g^{-1} - \tau_v^{-1})^{-1} < 0$ . The higher the value of  $K$ , the longer the duration of this plateau phase.

In order to exhibit the influence of the differential rotation on the  $r$ -mode evolution, for an example, we plot the  $r$ -mode evolution curves for  $K = 100$  (differential rotation case) and  $-2$  (non-differential rotation case) in Figure 2(a) for a comparison. As mentioned above, the non-differential rotation model ( $K = 2$ ) is incapable of determining a saturation amplitude. So, in the case of  $K = -2$ , we put an effective saturation amplitude by hand, which is taken to equal the one calculated from the contrastive differential rotation case for consistency (e.g.,  $\alpha_{sat} = 1.1$  for  $K = 100$ ). Correspondingly, Figures 2(b) and 2(c) show the temporal evolution of the stellar angular velocity and temperature, respectively, for both  $K = 100$  and  $-2$ . Especially, for the differential rotation case, we divide the stellar evolution

**Table 1** Different phases of the evolution of a young NS during the  $r$ -mode oscillation. The temporal behaviors of  $\alpha$ ,  $\Omega$ , and  $T$  are listed for every phase. The coefficient  $a = \frac{4}{3}(K + 2)Q\alpha_i^2$ .

Phases	I	II	IIIa	IIIb	IV	V
$\alpha(t) \propto$	$\exp(t/\tau_{g,i})$	$\exp(t/\tau_{g,i})$	$t^{1/10}$	$t^{1/10}$	$t^0$	decrease
$\Omega(t) \propto$	$t^0$	$1 - a \exp(2t/\tau_{g,i})$	$t^{-1/5}$	$t^{-1/5}$	$t^0$	increase
$T(t) \propto$	$t^{-1/6}$	$t^{-1/6}$	$t^{-1/6}$	$t^0$	$t^0$	decrease

during the  $r$ -mode oscillation into six phases (denoted by I-V) roughly, the temporal behaviors of which are listed in Table 1. Within phase IV, the slow changes of  $\Omega$  and  $T$  make the timescales  $\tau_g$  and  $\tau_v$  vary slowly. Thus, the simultaneous  $r$ -mode oscillation can maintain steady for a long period. Comparing the differential with non-differential rotation cases, we can find that: (1) The differential rotation obviously strengthens the gravitational braking effect for  $t < 0.1$  yrs (phases II and III). However, subsequently, from one tenth to a few thousand years (phases IV and V), the spindown of the star due to gravitational radiation would be held back effectively by an angular momentum transfer from  $J_r$  to  $I\Omega$ , although during this time the  $r$ -mode always stays in the saturation state. Due to the existence of this angular velocity plateau (i.e.,  $d\Omega/dt \sim 0$ ; phase IV), the star is expected to emit a quasi-monochromatic gravitational wave persistently. (2) The obvious difference in the temperature plateaus between the cooling curves with  $K = 100$  and  $-2$  indicates that the heating effect due to  $r$ -mode dissipation is also strengthened dramatically by the differential rotation. As a result, the NSs with differential rotation can keep a high constant temperature for a few thousand years. In view of the nearly constant temperature and angular velocity within phase IV, it is easy to understand the appearance of the steady  $r$ -mode saturation state. Finally, we also show the evolution trajectories of an isolated NS for  $K = 100$  and  $-2$  in the  $T - \Omega$  plane in Figure 3, where the six evolution phases defined for the differential rotation case are labelled. Especially, within phase V, a self-spinup of the differential-rotation star can be seen clearly. In addition, phase IV is marked by a solid circle, where a quasi-monochromatic gravitational wave could be emitted for a few hundred years (see Sect. 4).

To summarize, during the early part of the  $r$ -mode evolution (phases I, II, and III), the rotation energy of the star ( $\frac{1}{2}I\Omega^2$ ) is converted into the oscillation energy, the internal energy, and the energy of gravitational waves. In contrast, during the late part (phases IV and V), the energy deposited in the  $r$ -modes would be released gradually via heating the star and accelerating the stellar rotation due to viscosity. Moreover, this spin-up effect could be stronger than the gravitational braking effect.

### 3.3 NSs in LMXBs

For NSs in LMXBs, whose magnetic fields are usually found to be relatively weak ( $\sim 10^{8-9}$  G), their angular velocity could be increased by accreting materials from their companion star. Then, the evolution of the stellar angular momentum would be determined by the competition between the gravitational radiation and accretion as (Levin 1999; Zhang & Dai 2008)

$$\frac{dJ}{dt} = -\frac{3\alpha^2 \tilde{J} M R^2 \Omega}{\tau_g} + \dot{M} R^2 \Omega_K, \quad (19)$$

where  $\dot{M}$  is the accretion rate and the velocity of the accretion disk is assumed to equal the Keplerian velocity  $\Omega_K$ . Combining Eqs. (10) and (19), we can get

$$\frac{d\alpha}{dt} = \left[ 1 + \frac{4}{3}(K+2)Q\alpha^2 \right] \frac{\alpha}{\tau_g} - \left[ 1 + \frac{1}{3}(4K+5)Q\alpha^2 \right] \frac{\alpha}{\tau_v} - \frac{1}{\tilde{I}} \frac{\Omega_K}{\Omega} \frac{\alpha}{2\tau_a}, \quad (20)$$

$$\frac{d\Omega}{dt} = -\frac{8}{3}(K+2)Q\alpha^2 \frac{\Omega}{\tau_g} + \frac{2}{3}(4K+5)Q\alpha^2 \frac{\Omega}{\tau_v} + \left( \frac{1}{\tilde{I}} \frac{\Omega_K}{\Omega} - 1 \right) \frac{\Omega}{\tau_a}, \quad (21)$$

where  $\tau_a = M/\dot{M}$  is defined as an accretion timescale.

We plot in Figure 4 the evolution trajectories of an accreting NS in the  $T - \Omega$  plane for  $K = 100$  and  $-2$ . Different from the case of the isolated NS shown in Figure 3, the accreting star can be spun up by accretion significantly rather than spun down by magnetic dipole radiation in old age ( $\sim 10^{5-6}$  yrs). Especially, if the accretion rate is high enough, cyclic evolution could be found (black lines). This is qualitatively consistent with the results in Levin (1999) and Heyl (2002). However, for  $\dot{M} = 10^{-8} M_\odot \text{yr}^{-1}$  specifically, we do not obtain the cycle but Levin (1999) did. There are two reasons for this difference: (1) In the calculations of Levin (1999), an effective shear viscous damping timescale  $\tau_{sv} = 1.03 \times 10^6 T_9^2 \text{s}$  was taken by hand in order to fit the observed data, whereas we adopt a theoretical value of  $\tau_{sv} = 2.52 \times 10^8 T_9^2 \text{s}$  from Owen et al. (1998); (2) The cooling effect due to the thermal radiation, which can effectively pull the star away from the  $r$ -mode instability window in the  $T - \Omega$  plane, was ignored in Levin (1999).

The temporal behaviors of  $\alpha$ ,  $\Omega$ , and  $T$  within one cycle are exhibited in Figure 5. In order to show the detailed features of the cycle clearly, the time-axes in the left- and right-hand panels of Figure 5 are drawn on normal and logarithmical scales, respectively. To be specific, the left-hand panel shows that the period of the cyclic evolution is shortened by the differential rotation mildly ( $4.5 \times 10^5$  yrs vs  $5.6 \times 10^5$  yrs), and the right-hand panel indicates that the duration of the  $r$ -mode oscillation within one cycle is prolonged significantly (3,900 yrs vs 65 yrs). Similar to the early evolution of young NSs shown in Figure 2, the evolution during the  $r$ -mode oscillation within one cycle of the accreting NSs can be divided into five phases. A comparison between Figures 2 and 5 shows that the temporal behaviors of phases IIIb, IV, and V of young and accreting old NSs seems to be nearly identical except for their durations. This indicates that the isolated young and accreting old NSs may be able to produce some same astrophysical phenomena, e.g., self-spinup and persistent quasi-monochromatic gravitational wave radiation.

#### 4 DETECTABILITY OF GRAVITATIONAL WAVES FROM THE $R$ -MODE

Using the obtained  $r$ -mode amplitude and angular velocity, we can estimate the amplitude of the emitted gravitational waves as follows (Owen et al. 1998; Sá & Tomé 2006):

$$|h(t)| = 1.3 \times 10^{-24} \alpha(t) \left[ \frac{\Omega(t)}{\Omega_K} \right]^3 \left( \frac{20 \text{Mpc}}{d_L} \right), \quad (22)$$

where  $d_L$  is the distance of the star. Then, the frequency-domain gravitational wave amplitude [i.e., the Fourier transform of  $h(t)$ ,  $\tilde{h}(f) = \int_{-\infty}^{\infty} e^{2\pi i f t} h(t) dt$ ] can be calculated by (Owen et al. 1998; Sá & Tomé 2006)

$$|\tilde{h}(f)| = \frac{|h(t)|}{\sqrt{df/dt}}, \quad (23)$$

where  $f = 2\Omega/(3\pi)$  is the frequency of the gravitational waves. In order to analyze the possibility of detecting the gravitational waves with laser interferometer detectors LIGO and Virgo, in Figure 6 we compare the characteristic amplitude of the signal,  $h_c(f) = f|\tilde{h}(f)|$ , with the rms strain noise in the detectors,  $h_{\text{rms}}(f) = \sqrt{f S_h(f)}$ , for both isolated (left-hand panel) and accreting (right-hand panel) NSs. For the noise spectral density of the detectors,  $S_h(f)$ , some approximative expressions can be found for LIGO, Virgo, and advanced LIGO in Sá & Tomé (2006).

On one hand, as found by Sá & Tomé (2006), the spike of  $h_c(f)$  at  $f_{\text{max}} = 2\Omega_K/(3\pi)$  that was predicted by Owen et al. (1998; see the thick dashed lines in Figure 6) disappears under the influence of the differential rotation, and the numerical results of  $h_c(f)$  for  $f > 100$  Hz in Figure 6 can be fitted by the following analytical expression perfectly

$$h_c(f) = \frac{5.5 \times 10^{-22}}{\sqrt{K+2}} \sqrt{\frac{f}{f_{\text{max}}}} \left( \frac{20 \text{Mpc}}{d_L} \right). \quad (24)$$



**Table 2** Signal-to-noise ratio of gravitational wave detections for different detectors, different values of  $K$ , and different detection duration for an isolated NS at  $d_L = 20$  Mpc. The begin of the detection is set at the birth of the star.

$t_{\text{det}} - t_0$	LIGO			Virgo			advanced LIGO		
	$K = 1$	10	100	1	10	100	1	10	100
0.3 yrs	0.65	0.33	0.11	0.51	0.26	0.01	9.18	4.62	1.59
1 yrs	0.67	0.34	0.12	0.54	0.27	0.01	9.63	4.90	1.69
10 yrs	0.81	0.44	0.15	0.77	0.42	0.15	13.53	7.46	2.63
30 yrs	0.91	0.55	0.20	1.06	0.62	0.22	18.60	10.98	3.93

On the other hand, surprisingly, a new remarkable spike emerges within the range of  $\sim 60 - 90$  Hz, where the approximative analysis in Sá & Tomé (2006) is inapplicable. From Figures 2 and 5 we know that, during phase IV, the angular velocity of the star can nearly keep constant (i.e.,  $|df/dt| \rightarrow 0$ ) over a few hundred years, while the  $r$ -mode stays in the saturation state all the time. As a result, a quasi-monochromatic gravitational wave could be emitted from both young and accreting old NSs, which lasts a few hundred years. Additionally, for accreting NSs, another weaker spike at  $\sim 220$  Hz is predicted due to the existence of Phase I'.

Using matched filtering, the power signal-to-noise ratio  $(S/N)^2$  of a detection from  $t_0$  to  $t_{\text{det}}$  is given by (Owen et al. 1998; Sá & Tomé 2006)

$$\left(\frac{S}{N}\right)^2 = 2 \int_{t_0}^{t_{\text{det}}} \left[ \frac{f(t)h(t)}{h_{\text{rms}}(f(t))} \right]^2 dt, \quad (25)$$

where  $t_0$  is determined by the begin of the detection. In Table 2, we list some values of  $S/N$  with different  $t_{\text{det}}$  and  $K$  for an isolated NS by setting  $t_0$  at the birth of the star. Since the spike of  $h_c(f)$  within  $\sim 60 - 90$  Hz would appear about 0.3 yrs later after the rising of the  $r$ -modes, the signal-to-noise ratio obtained from a long-term detection could be much higher than that from a short-period detection (i.e., the case focused in Sá & Tomé 2006).

## 5 SUMMARY AND DISCUSSION

A second-order  $r$ -mode theory was developed by Sá & Tomé (2004; 2005). This theory predicts that  $r$ -mode oscillation could induce differential rotation in neutron stars, which can determine a saturation amplitude of the  $r$ -mode spontaneously. In the framework of this theory, we investigate the long-term spin and thermal evolutions of isolated NSs and NSs in LMXBs. In our calculations, the effects of heating due to  $r$ -mode dissipation, gravitational and magnetic braking, and accretion are taken into account. Our results show that, to a certain extent, the linear  $r$ -mode evolution model using an artificial saturation amplitude can describe the basic features of the evolution of NSs qualitatively, but predicts an obviously underestimated  $r$ -mode duration. By considering the differential rotation, we may obtain a slight self-spinup and an enhanced temperature plateau for NSs. Especially, due to the effective angular momentum transfer from  $J_r$  to  $I\Omega$ , the spindown of the NSs can be stopped for a few hundred years, whereas the gravitational radiation still exists during this period. As a result, long-lasting quasi-monochromatic gravitational wave radiation is predicted, which increases the detectability of gravitational waves from both nascent and accreting old ( $\sim 10^{5-6}$  yrs) NSs.

In this paper, we adopt a very simple NS model just in order to find the influences of nonlinear effects on the evolution of NSs qualitatively. However, generally speaking, NSs are probably hybrid stars or even strange quark stars. The former undergoes a deconfinement transition from neutron matter to quark or hyperon matter (Glendenning 1997; Pan et al. 2006), and the latter consists of nearly pure quark matter (Alcock et al. 1986; Zheng et al. 2006). It is a demanding task to study the  $r$ -mode evolution in a more realistic NS model. Especially, for a hybrid star that contains a quark or hyperon core, since

the direct Urca is triggered and superfluidity exists, the star without reheating would have a very low temperature that is inconsistent with the observational data. So, it may be helpful for enhancing the temperature of the hybrid stars to consider the heating effect due to  $r$ -mode dissipation.

**Acknowledgements** This work is supported by the National Natural Science Foundation of China (grant nos. 10603002 and 10773004). YWY is also supported by the Scientific Innovation Foundation of Huazhong Normal University.

## References

- Alcock C., Farhi E., & Olinto A., 1986, *ApJ*, 310, 261  
 Andersson N., 1998, *ApJ*, 502, 708  
 Arras, P., Flanagan, E. E., Morsink, S. M., Schenk, A. K., Teukolsky, S. A., Wasserman, I. 2003, *ApJ*, 591, 1129  
 Brink, J., Teukolsky, S. A., Wasserman, I. 2004a, *Phys. Rev. D*, 70, 121501  
 Brink, J., Teukolsky, S. A., Wasserman, I. 2004b, *Phys. Rev. D*, 70, 124017  
 Brink, J., Teukolsky, S. A., Wasserman, I. 2005, *Phys. Rev. D*, 71, 064029  
 Chandrasekhar S., 1970, *Phys. Rev. Lett.*, 24, 611  
 Friedman J. L. & Morsink S. M., 1998, *ApJ*, 502, 714  
 Friedman J. L. & Schutz B. F., 1978, *ApJ*, 221, 937  
 Gudmundsson E. H., Pethick C. J., & Epstein R. I., 1983, *ApJ*, 272, 286  
 Glendenning, N.K., 1997, *Compact Stars* (Springer-verlag)  
 Heyl J. S., 2002, *ApJ*, 574, L57  
 Ho W. C. G. & Lai D., 2000, *ApJ*, 543, 386  
 Levin Y., 1999, *ApJ*, 517, 328  
 Lindblom L., Owen B. J., & Morsink S. M., 1998, *Phys. Rev. Lett.*, 80, 4843  
 Lindblom L., Tohline J. E., & Vallisneri M., 2001, *Phys. Rev. Lett.*, 86, 1152  
 Owen B. J., Lindblom L., Cutler C., Schutz B. F., Vecchio A., Andersson N., 1998, *Phys. Rev. D*, 58, 084020  
 Pan N. N., Zheng X. P., & Li J. R., 2006, *MNRAS*, 371, 1359  
 Rezzolla L., Lamb F. K., & Shapiro S. L., 2000, *ApJ*, 531, L139  
 Rezzolla L., Lamb F. K., Frederick K., Markovic D., & Shapiro S. L., 2001, *Phys. Rev. D*, 64, 104013  
 Sá P. M., 2004, *Phys. Rev. D*, 69, 084001  
 Sá P. M. & Tomé B., 2005, *Phys. Rev. D*, 71, 044007  
 Sá P. M. & Tomé B., 2006, *Phys. Rev. D*, 74, 044011  
 Schenk, A. K., Arras, P., Flanagan, É. É., Teukolsky, S. A., Wasserman, I. 2002, *Phys. Rev. D*, 65, 024001  
 Shapiro S. L. & Teuklosky S. A., 1983, *Black holes, white dwarfs and neutron stars* (New York, Wiley)  
 Stergioulas N. & Font J. A., 2001, *Phys. Rev. Lett.*, 86, 1148  
 Watts A. L. & Andersson N., 2002, *MNRAS*, 333, 943  
 Yakovlev D. G., Levenfish K. P., & Shibano Yu. A., 1999, *Phys. Usp.*, 42, 737 [arXiv: astro-ph/9906456]  
 Yakovlev D. G. & Pethick C. J., 2004, *ARA&A*, 42, 169  
 Zhang D. & Dai Z. G., 2008, *ApJ*, 683, 329  
 Zheng X. P., Yu Y. W., & Li J. R., 2006, *MNRAS*, 369, 376



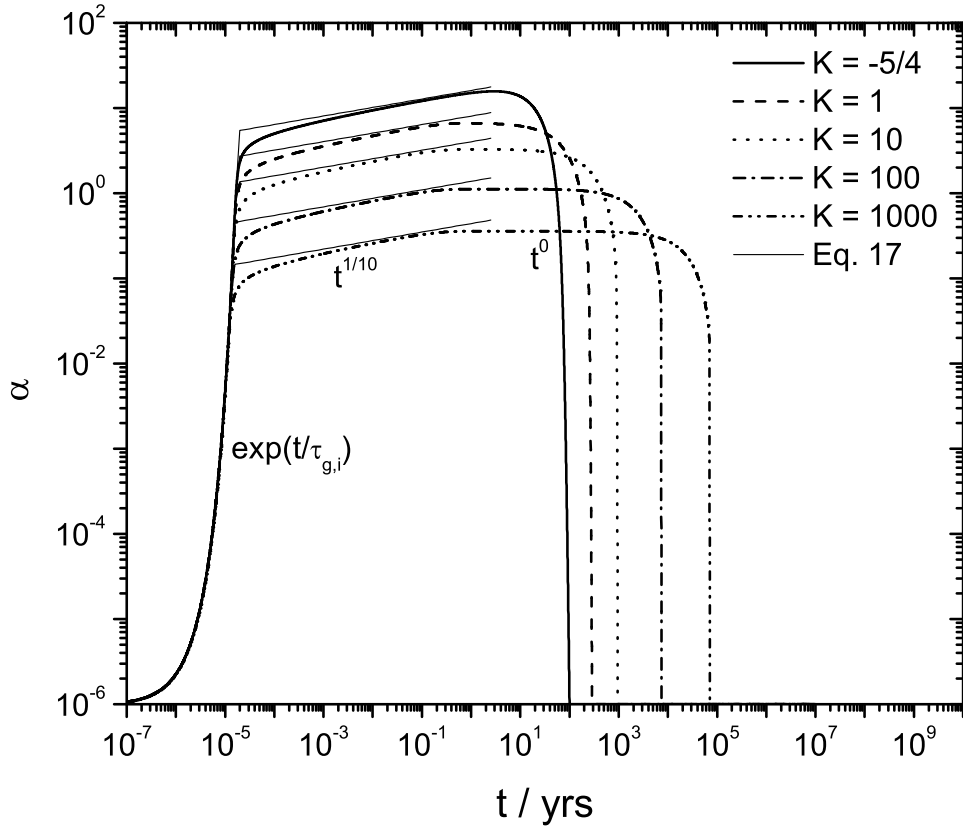


**Fig. 1** Evolution of  $r$ -mode amplitude of an isolated NS with a magnetic field  $B = 10^{12}\text{G}$  for different values of  $K$  (thick lines). The thin solid lines are given by the asymptotic functions shown in Eq. (17). The initial values of the  $r$ -mode amplitude, angular velocity, and temperature are taken to be  $\alpha_i = 10^{-6}$ ,  $\Omega_i = \Omega_K \equiv \frac{2}{3}\sqrt{\pi G \bar{\rho}}$ , and  $T_i = 10^{10}\text{K}$ , respectively, where  $\Omega_K$  is the Keplerian angular velocity at which the star starts shedding mass at the equator.

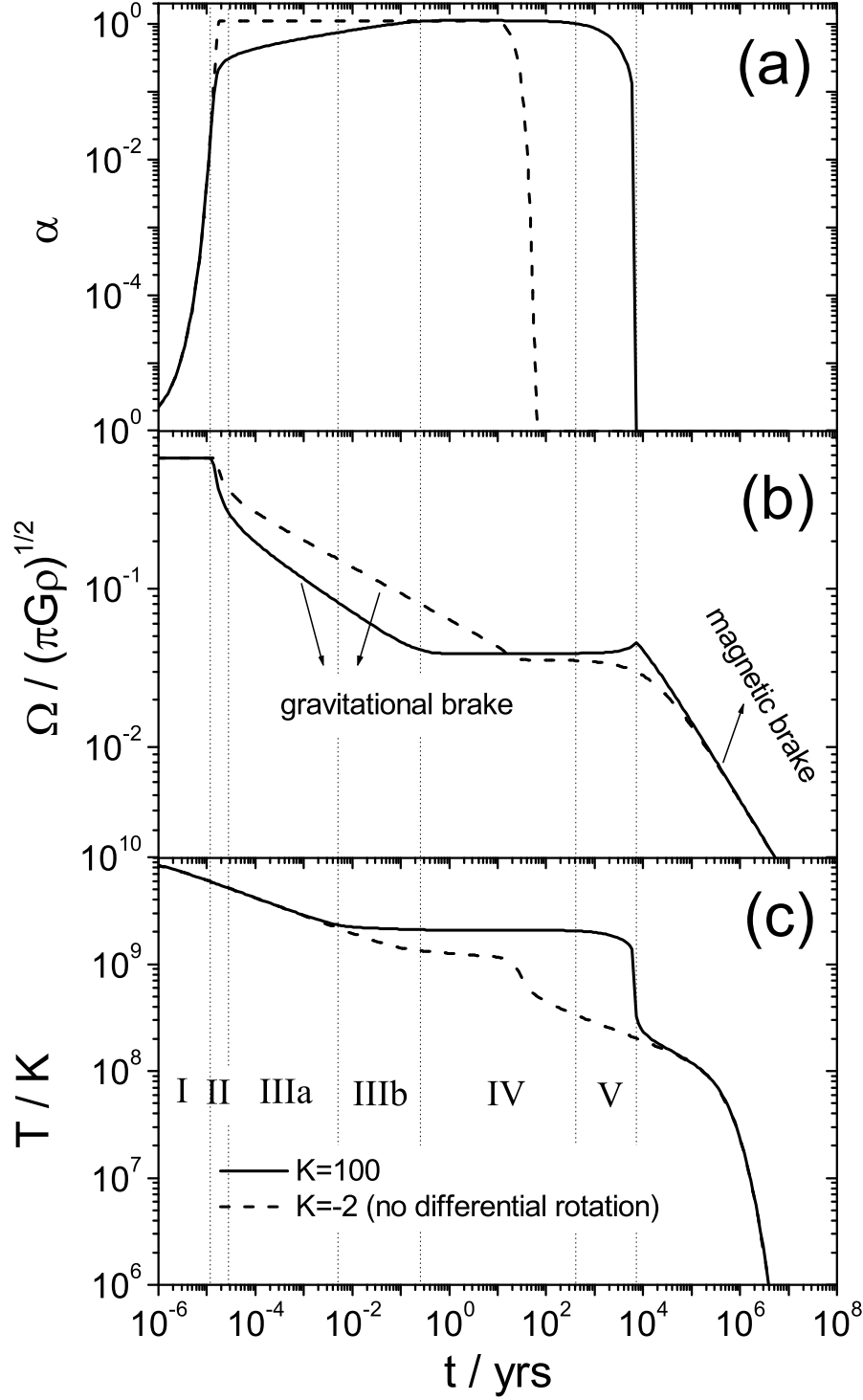


**Fig. 2** Evolution curves of  $\alpha$ ,  $\Omega$ , and  $T$  of an isolated NS with a magnetic field  $B = 10^{12}$  G for  $K = 100$  (solid lines; differential rotation case) and  $K = -2$  (dashed lines; non-differential rotation case). The initial conditions are the same to that in Figure 1. The evolution during the  $r$ -mode oscillation is divided into several phases (denoted by I-V) by the vertical dotted lines.

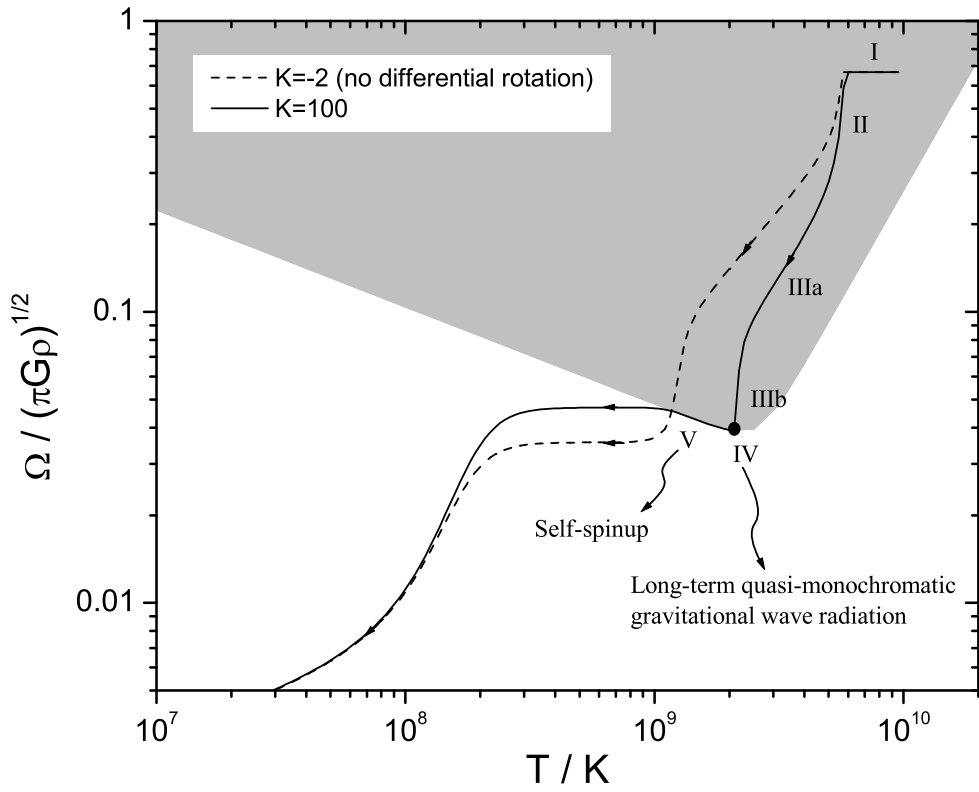


**Fig. 3** Evolution trajectories of an isolated NS with  $B = 10^{12}$  G in the  $T - \Omega$  plane for  $K = 100$  (solid line; differential rotation case) and  $K = -2$  (dashed line; non-differential rotation case). The initial conditions and the meaning of phases I-V are the same to that in Figure 1. The shaded region exhibits the  $r$ -mode instability window.

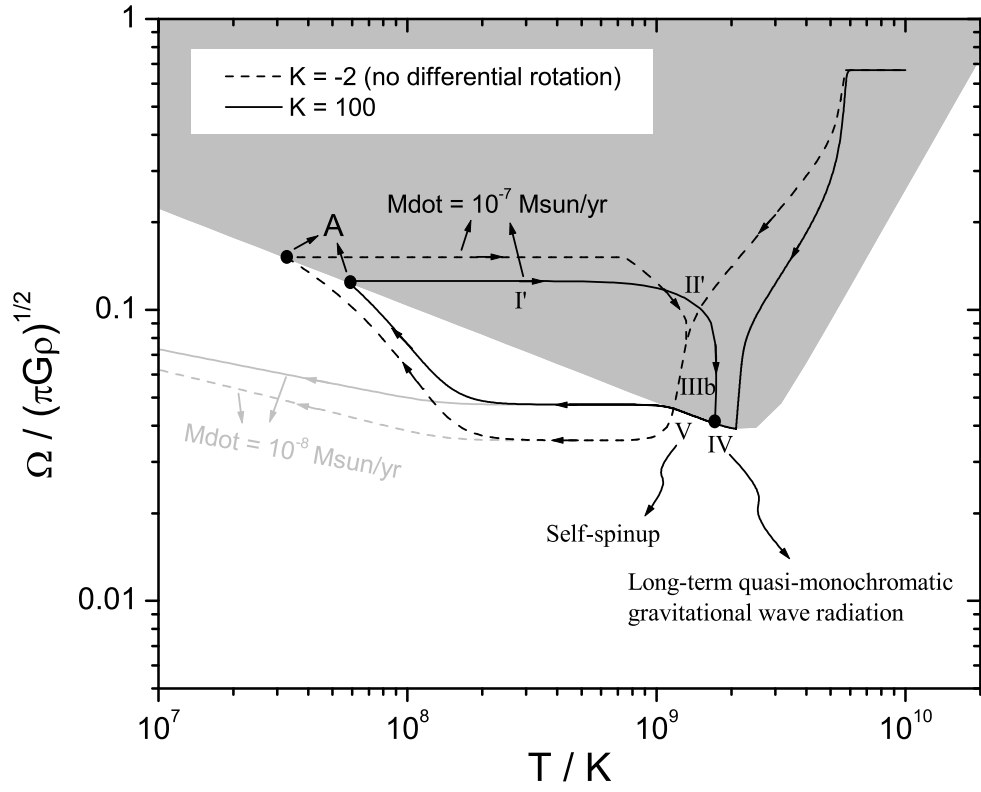


**Fig. 4** The same to Figure 3 but for a NS with  $B = 10^8$  G in a LMXB. The black and grey lines correspond to the accretion rates  $\dot{M} = 10^{-7} M_{\odot} \text{yr}^{-1}$  and  $10^{-8} M_{\odot} \text{yr}^{-1}$ , respectively.

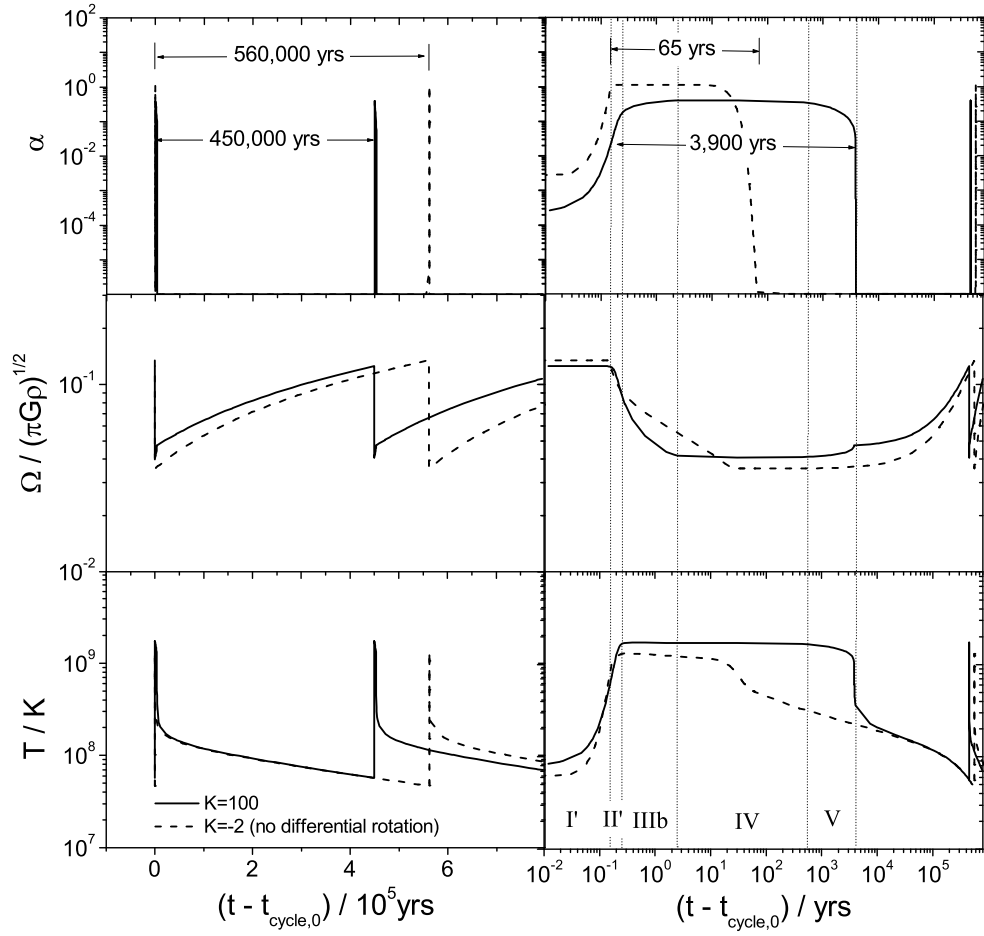


**Fig. 5** Evolution curves of  $\alpha$ ,  $\Omega$ , and  $T$  during the cyclic evolution of a NS with  $B = 10^8$  G in a LMXB for  $K = 100$  (solid lines; differential rotation case) and  $K = -2$  (dashed lines; non-differential rotation case). The begin of the cycle is set at point A that is marked in Figure 4, and the age of the star at point A is denoted by  $t_{\text{cycle},0}$ .

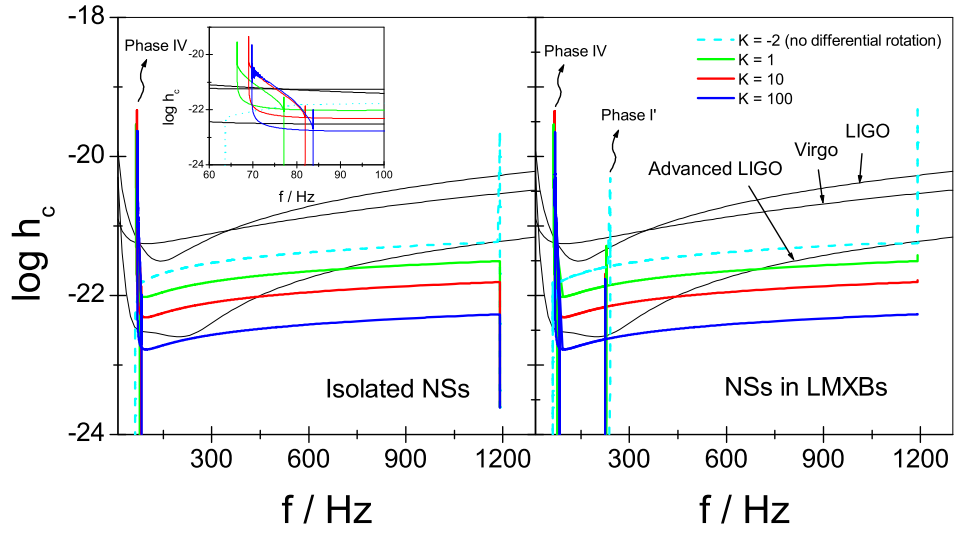


**Fig. 6** A comparison of the characteristic amplitude of gravitational waves for different values of  $K$  (thick lines) with the rms strain noise in the detectors (thin solid lines). The details of the spike of  $h_c$  within  $\sim 60 - 90$  Hz is shown in the insert panel.